Formation of Stable Polypeptide Monolayers at Interfaces: Controlling Molecular Conformation and Orientation

Mila Boncheva and Horst Vogel
Institute of Physical Chemistry, Swiss Federal Institute of Technology, Lausanne, Switzerland

ABSTRACT The molecular self-organization and structural properties of peptide assemblies at different interfaces, using either amphipathic or hydrophobic polypeptide helices, is described. The two peptides under investigation form stable monolayers on the water surface under the conservation of their molecular conformation, as studied by circular dichroism and polarization-modulation Fourier transform infrared (FTIR) spectroscopy. Using surface plasmon resonance and reflection-absorption FTIR, we show that such molecular layers can be transferred unaltered to solid substrates. Most importantly, the molecular orientation of the hydrophobic helices on solid supports such as gold can be controlled by choosing a particular procedure for the layer formation. The helices were oriented parallel to the interface in Langmuir-Blodgett monolayers, and perpendicular to the interface in self-assembled monolayers. Our reflection-absorption FTIR measurements have delivered for the first time direct experimental evidence for the molecular conformation and orientation of pure peptide monolayers. Suitable reference spectra of polypeptides with defined conformation and orientation are necessary to use this technique for the determination of the molecular orientation of peptides in monomolecular films. We have solved the problem for α-helical polypeptides by using bacteriorhodopsin as a reference in combination with synthetic α-helices of defined interfacial orientation. The present study shows the possibility of constructing immobilized peptide monolayers with predefined macroscopic properties and molecular structure by choosing the proper polypeptide amino acid sequence, the technique used for layer formation, and the supporting surface properties.

INTRODUCTION

Molecular self-organization can be defined as the spontaneous association of molecules into stable, structurally well-defined aggregates joined by noncovalent bonds (Kuhn, 1989; Prime and Whitesides, 1991; Ulman, 1991). This process is driven by one or several interactions between the participating molecules, such as steric, electrostatic, van der Waals, or hydrophobic contributions. Molecular self-organization processes play important roles in many different areas. For example, the formation of biological structures on a molecular and on a cellular level often originates from specific molecular interactions and self-organization reactions. The understanding of these complex processes belongs to the central issues in biological sciences, but the knowledge obtained from natural systems can lead to a tremendous benefit in technical applications such as modified surfaces, novel materials, electrochemistry, electronics microfabrication, sensor technology, and nanotechnology, to mention a few (Drexler, 1992; Fendler, 1994; Urry, 1993).

Much effort has been applied during the last decades to understanding the process of molecular self-organization of amphipathic molecules comprising long-chain hydrocarbons, such as fatty acids, lipids, and a multitude of derivatives thereof (Boncheva et al., 1996; Duschl et al., 1996; Mrksich and Whitesides, 1996; Schmitt et al., 1996; Ulman, 1991). Surprisingly, the structural and functional versatility of peptides and their potential for the formation of supramolecular structures by self-assembly and self-organization have up to now been largely neglected, with a few exceptions (Fujita et al., 1995; Ghadiri and Case, 1993; Schwarz and Taylor, 1995; Whitesell et al., 1994). Amphipathic polypeptides in particular offer a large potential for the controlled formation of self-organized monomolecular layers at interfaces. By proper choice of the amino acid sequence, it is possible to create tailor-made peptide layers of predefined molecular conformation (α-helix, β-strand), orientation, and flexibility.

The general concept of peptide layer formation used in the present work is outlined in Fig. 1. Shown are polypeptides at the interface between two phases which, under experimental conditions, can be air and water (as in the case of Langmuir monolayers), or a fluid phase (water, organic solvent) in contact with a solid surface (as in the case of self-assembly on solid supports), or an air-solid interface (as in the case of peptide layers formed by transfer of Langmuir monolayers to suitable supports). Polypeptides of two different molecular structures are of primary interest: α-helices and β-strands. In both cases, the principal molecular axis can be oriented either perpendicularly to or in the plane of the interface, in parallel or in antiparallel intermolecular arrangement. By changing the angle between the molecular axes and the interface, formation of intermediates between the perpendicular and in-plane orientations is possible. The central question in this context is how to control the particular structure of the peptide layer, i.e., the conformation

Received for publication 18 February 1997 and in final form 8 May 1997.
Address reprint requests to Dr. Horst Vogel, EPFL-LCPPM, CH-1015 Lausanne, Switzerland. Tel.: 41-21-6933155; Fax: 41-21-6936190; E-mail: horst.vogel@icp.dc.epfl.ch.

0006-3495/97/08/1056/17 $2.00

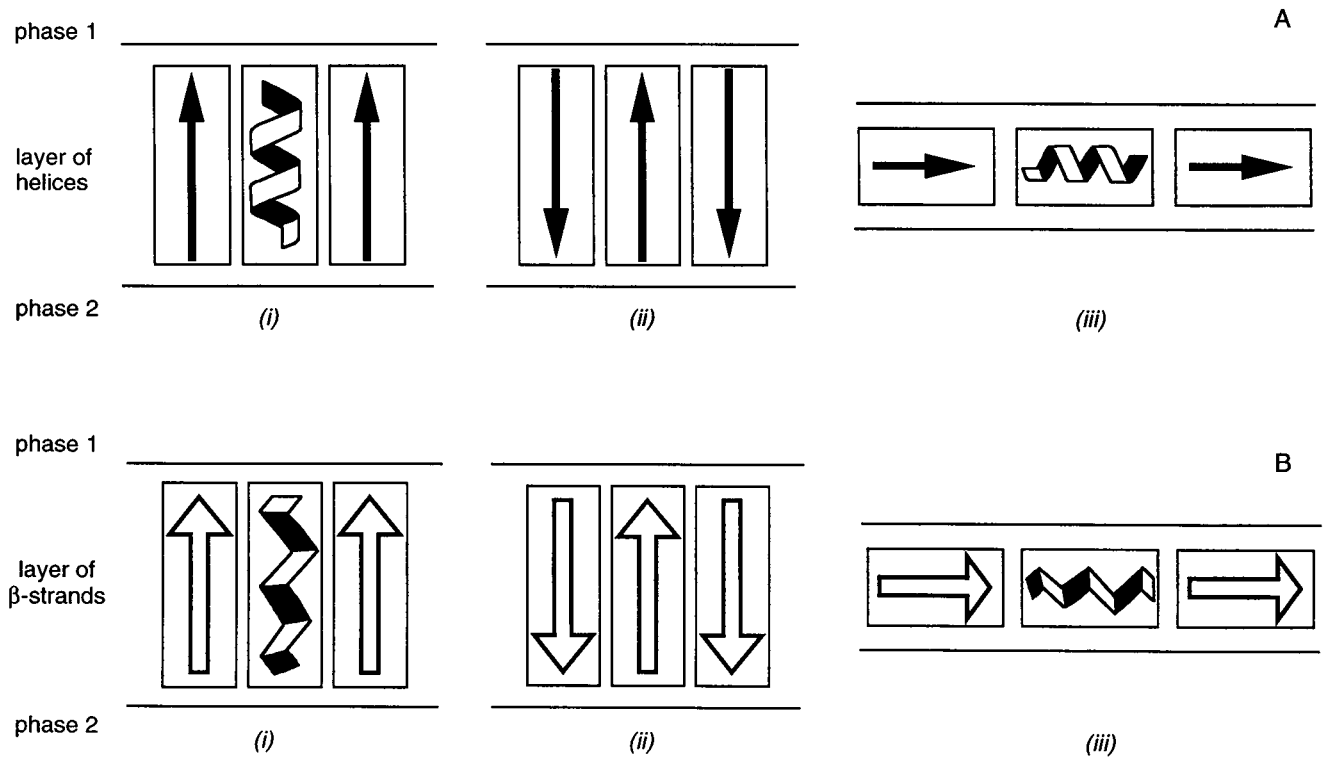

FIGURE 1 General concept for peptide layer formation at the interface between two different phases (1 and 2), for helical (*A*) and β-stranded (*B*) peptides. The rectangles represent peptide molecules, densely packed as monomolecular films. Within the rectangles the two peptide structures are depicted: in the top row, helical polypeptides, shown either as a schematic helix or as bold arrows indicating the molecular direction from the N to the C terminus; in the bottom row, β-stranded polypeptides, shown either as a schematic folded strand, or as unfilled arrows, again indicating the molecular direction. For both peptide conformations, three different molecular orientations in the monolayer are shown: peptides with their principal axes perpendicularly oriented to the interface with either parallel (*i*) or antiparallel (*ii*) intermolecular alignment, and peptides lying flat between the phases (*iii*). The phases 1 and 2 can be air and water, as in the case of Langmuir film balance, or water and solid support, as in the case of supported peptide monolayers.

and orientation of the individual peptide molecules at the interface.

The requirements for the formation of α-helical peptide conformation in solution were elucidated in detail recently and, to a lesser extent, for the formation of β-structures (Chakrabartty et al., 1991; DeGrado and Lear, 1990; Lyu et al., 1990; Minor and Kim, 1994; Ghadiri and Case, 1993; Schneider and Kelly, 1995; Tuchscherer and Mutter, 1995). The formation of regular peptide structures in solution is driven by competition between intramolecular peptide and peptide-solvent interactions. In the case of regular, self-organized peptide layers, additional components such as peptide-peptide and peptide-interface interactions come into play.

Once a suitable sequence for a regular peptide structure is chosen, the molecular orientation of the peptides at the interface may be controlled by mutual interactions between hydrophilic (electrically neutral or charged) and hydrophobic molecular surfaces of neighboring peptides and the interfacial region such as the surface of a solid support. To control the direction of the molecules at the interface, particularly in the case of self-assembly at solid surfaces, specific binding reactions between functional groups of the peptide and the support may be important. Examples are the binding of sulfur-containing molecules to gold or silver surfaces, the selective binding of histidine to NTA-covered surfaces via metal chelates, or biotin-avidin interactions.

The two polypeptides used in the present study are presented in Fig. 2. The particular amino acid sequences were chosen to create hydrophobic (A-peptide) or amphipathic (His-peptide) α-helices, and to enable their regular organization at the air/water interface and on solid surfaces. The inclusion of the sulfur-bearing Cys residue at either the N- or C-terminus should direct the molecules uniformly toward gold surfaces during monolayer formation by self-assembly. In the A-peptide, the nonnatural amino acid T($\Psi^{H,H}$pro) (pseudo-proline), was introduced at position 15 to facilitate the chemical synthesis of this rather long, hydrophobic molecule (Wöhr et al., 1996). Like proline, pseudo-proline introduces a kink into an otherwise regular helical structure.

Within the conceptual framework of peptide layer formation, the present work concentrates on the following questions: 1) Do the two peptides under investigation form stable peptide layers on the water surface under conservation of their molecular conformation in bulk solutions? 2) Can the molecular layers be transferred to solid substrates while conserving their molecular structures? 3) Is it possible to control the formation of different molecular structures of

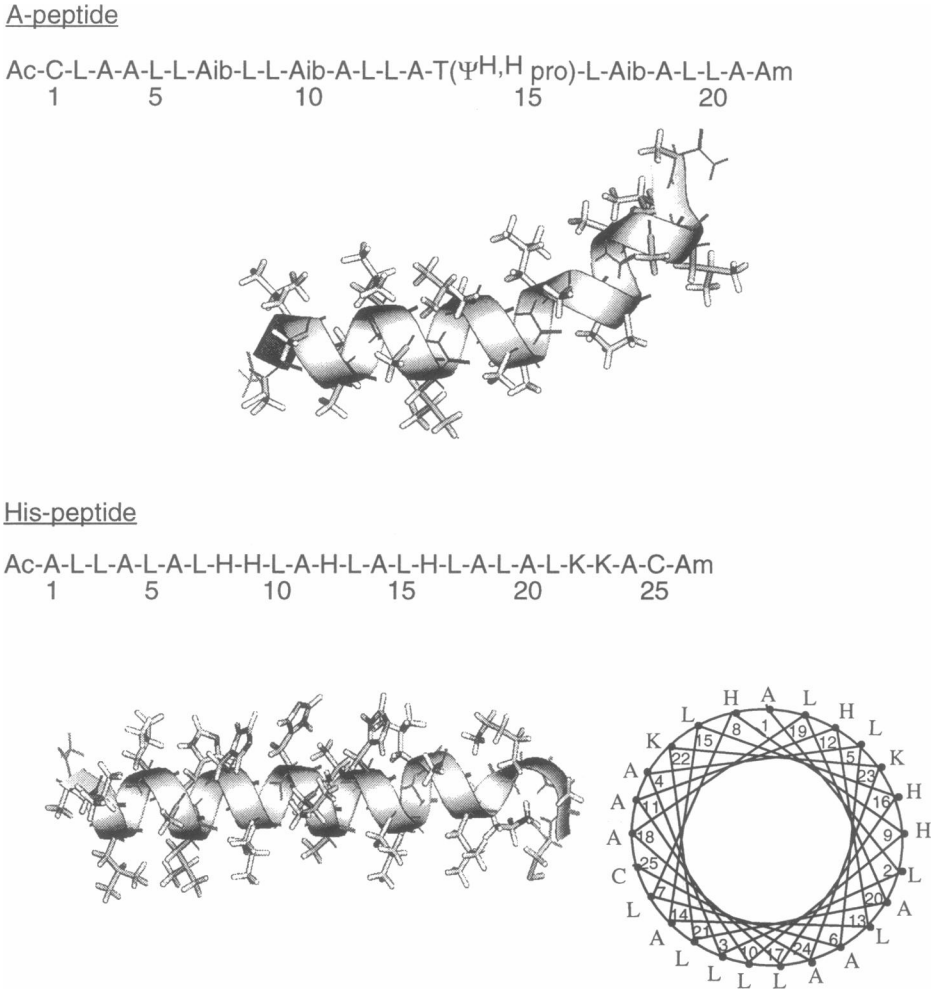

FIGURE 2 Amino acid sequence and helical structure of the A-peptide and the His-peptide, both acetylated at the N-termini and amidated at the C-termini. Both peptides form stable helices. The corresponding three-dimensional structures are shown in the helical ribbon representation as a result of a 1-ns MD simulation. For the A-peptide, T($\Psi^{H,H}$pro) was replaced by proline, which induced a kink at amino acid positions 10–11. The His-peptide remained a stable, straight α-helix during the whole simulation time span. The amphipathic nature of this peptide is clearly visible in the helical wheel representation, showing an ideal segregation of hydrophobic and hydrophilic amino acid residues on opposite helix surfaces. The molecular dimensions of the peptides calculated from the mean values of the atomic coordinates during the last 20 ps of the MD trajectory are: His-peptide: 37 Å, length of the peptide helix; 12 Å, helix diameter (including the side chains); A-peptide: 15.1 Å, length of the helix segment comprising residues 1–10; 16.7 Å, length of the helix segment comprising residues 11–21; 11 Å, helix diameter (including the side chains); angle induced by the nonnatural amino acid T($\Psi^{H,H}$pro), (pseudo-proline), 147° ± 9° (mean value from the whole trajectory).

supported peptide layers using different self-organization processes such as self-assembly and LB transfer?

To address these particular questions, a combination of surface-sensitive techniques were applied that delivered detailed information on the molecular structure of the peptide layers at different types of interfaces. First of all, the average conformation of the two peptides was investigated by circular dichroism (CD) and infrared spectroscopy for comparative purposes. The question of the properties of the polypeptides at the air-water interface was investigated by the Langmuir monolayer technique, yielding information on the molecular dimensions, compressibility, and phase behavior of the peptide monolayers. Furthermore, by applying polarization modulation Fourier transform infrared (FTIR) reflection absorption spectroscopy (PM-IRRAS) to peptide monolayers on the Langmuir film balance, it was possible to determine the molecular conformation and orientation of the polypeptides at the water surface under different experimental conditions, such as surface area and lateral pressure. Finally, a combination of surface plasmon resonance (SPR) and reflection-absorption FTIR (RA-FTIR) measurements revealed the properties of the peptide layers on solid supports. SPR yielded data on the molecular density of the supported peptide layers, whereas RA-FTIR spectroscopy delivered details on the peptide molecular conformation and orientation.

In the context of the central issues of the present work, a technical problem was solved that is of general importance for the application of the RA-FTIR technique to elucidate the structure of ultrathin peptide layers. Suitable reference spectra of polypeptides with defined conformation and orientation are necessary to use this technique to determine the molecular orientation of peptides in monomolecular films. We have solved the problem for α-helical polypeptides by using bacteriorhodopsin (BR) as a reference in combination with synthetic α-helices of defined interfacial orientation.

MATERIALS AND METHODS

The A-peptide was synthesized by Dr. T. Sato (Institut de Chimie Organique, Université de Lausanne, Lausanne, Switzerland). The His-peptide was a gift from Dr. B. Bechinger (Max-Planck-Institut für Biochemie, Martinsried, Germany). Both peptides were synthesized by automated solid-phase synthesis, using Fmoc chemistry as described elsewhere (Bechinger, 1996; Wöhr et al., 1996). They were stored as dry powders at −20°C and dissolved before use to give stock solutions of 1 mg/ml in methanol/dichloromethane (1:9). The solutions were stored at 4°C. The exact peptide

concentration was determined by amino acid analysis. The purple membranes were a gift from Dr. W. Gärtner (Max-Planck-Institut für Strahlenforschung, Mülheim, Germany), and were prepared as described elsewhere (Vogel and Gärtner, 1987).

The organic solvents and the salts were purchased from Fluka (Buchs, Switzerland), and were of the best quality available. The water used in all experiments was purified in an ion-exchanger purification train (Milli-Q System; Nanopore, Volketswil, Switzerland) and had a resistivity higher than 18 MΩ cm.

Peptide monolayers

For the monolayer experiments we used a computer-controlled Langmuir film balance (Riegler and Kirstein, Mainz, Germany). The trough and the barriers were made of Teflon, and the pressure was measured via Wilhelmy plate. The peptide monolayers were spread on the water surface from methanol/dichloromethane solutions (1:9) using a Hamilton microsyringe. After solvent evaporation (10–15 min), the monolayers were compressed at a speed of 0.05 nm^2 $molecule^{-1}$ min^{-1}. Unless otherwise indicated, the subphase temperature was kept constant at 22 ± 2°C. The phase behavior of the peptide monolayers during compression was followed with a Brewster angle microscope (BAM2; Nanofilm Technology, Göttingen, Germany). The pH dependence of the His-peptide isotherms was studied using the same film, to avoid possible errors in the molecular area determination. The monolayer was spread first on 100 ml aqueous buffer of 0.025 M glycine/NaOH, pH 9. After a compression/expansion cycle, the pH of the bulk buffer phase was changed to 3 by injecting 50 μl of concentrated HCl and stirring with a small magnetic bar placed on the trough bottom.

Surface plasmon resonance

The SPR experiments were performed on a home-built set-up in the Kretschman configuration as previously described (Terretaz et al., 1993). In the presence of an organic layer at the metal/dielectric interface, the position of the resonance angle (θ^{spr}) shifts to higher values. The measurement of $\Delta\theta^{spr}$ allows the determination of the optical thickness of the adsorbed layer by using the relation $\Delta\theta^{spr} = k\Delta nd$, where k is a constant reflecting the experimental conditions, d is the geometrical thickness of the organic layer, and Δn is the difference between the real refractive indices of the layer and the medium.

To calculate the mass coverage in the peptide layers, we used as a first approximation a value for the layer refractive index of $n = 1.45$ (Duschl et al., 1996). Thus an angle shift of 1° corresponds to a layer thickness $d_{1.45}$ of 6.4 nm. The mean molecular area A_{SPR} of the peptides in the layer was calculated as $A_{SPR} = (m\ dn/dn)/(d_{1.45}\Delta n)$, where m is the mass of the corresponding peptide molecule (4.43×10^{-21} g for the His-peptide, and 3.46×10^{-21} g for the A-peptide), and $dn/dc = 0.18$ cm^3g^{-1} is the refractive index increment (Sober, 1973; Brandrup and Immergut, 1989). An estimation of the actual monolayer thickness d that is more realistic and independent of the chosen n value was obtained by using a typical peptide density $\rho = 1.37$ g/cm^3 (Gennis, 1989) as $d = m/(A_{SPR}\rho)$.

The real refractive index of the peptide layers was then calculated by fitting the experimental reflectivity versus angle of incidence scans with the Fresnel equations and using the above-calculated d.

Sample preparation

Glass slides (9 cm^2, glass type SF10, $n = 1.730 \pm 0.005$; Guinchard, Yverdon-les-Bains, Switzerland) were cleaned by ultrasonication in detergent (Hellmanex; Hellma, Müllheim, Germany) and water. Chromium and gold films (thickness 4 nm and 45 nm, respectively) were consecutively evaporated on a glass slide in a vacuum chamber at 5×10^{-6} mbar. The sample was optically matched to the base of a 60° glass prism (SF10; Spindler and Hoyer). It was pressed onto a Teflon support to form a reaction cell of 300 μl. After determination of the resonance angle on the bare gold surface, peptide layers were formed by self-assembly (SA) from organic solution, horizontal Langmuir-Schäfer (Langmuir and Schäfer, 1938), or standard Langmuir-Blodgett (LB) transfer of preformed monolayers on water compressed to the desired surface pressure. The transfer ratios (defined as the ratio between the area change of the monolayer during the transfer at constant surface pressure and the geometrical area of the withdrawn substrate) were close to 1 in all cases. Subsequent angle scans gave the angle shifts, which allowed determination of the optical film parameters.

FTIR spectroscopy

FTIR measurements of the peptides in organic solution (methanol/dichloromethane = 1:9) and immobilized on solid supports (Ge and Au) were performed with an IFS 66 Equinox spectrometer (Bruker, Germany). The spectra in solution were recorded with a DTGS detector in a cell with CaF_2 windows, and a path length of 60 μm. A thousand scans were taken with a resolution of 4 cm^{-1} and averaged for each measurement. The spectra were corrected for the solvent absorption. Absorbance spectra of the peptides as bulk solid samples were obtained in a conventional transmission mode by drying an organic solution on BaF_2 windows. The attenuated total internal reflection (ATR) and RA-FTIR measurements (angle of incidence 45° and 85°, respectively) were performed with an HgCdTe detector. Typically, 1000 scans were recorded at a frequency of 80 kHz, with a resolution of 1 cm^{-1}, a boxcar apodization, and a level of zero-filling equal to 1. Background spectra of the bare supports were recorded before layer formation in each experiment and subsequently subtracted from the particular sample spectra. For the precise subtraction of spectral contribution from the water vapor, we employed the procedure described by Goormaghtigh et al. (1994b). The decomposition of the amide I and amide II spectral regions into individual bands was performed with the OPUS software, version 2.0 (Bruker), supplied with the spectrometer. The 1500–1800 cm^{-1} regions of the spectra were analyzed as a sum of Gaussian/Lorentzian curves with the Levenberg-Marquardt algorithm, with consecutive optimization of the amplitudes, band positions, half-widths, and Gaussian/Lorentzian composition of the individual bands. The quadratic deviation for all fits presented here was less than 5×10^{-5}. The positions and the relative intensities of these bands were used to determine the secondary structure of the peptides and their molecular orientation with respect to the interface.

Sample preparation

Supported peptide layers were prepared by using either the standard LB transfer or SA from organic solution. LB transfer of peptide monolayers was performed at surface pressures of 8 and 30 mN/m. For the SA, gold-covered glass slides (gold thickness ≥ 100 nm) were incubated for 2 h in the organic peptide solution, followed by extensive washing with the solvent and drying in a stream of nitrogen. Planar layers of bacteriorhodopsin were prepared by spreading a 20-μl purple membrane suspension in water (optical density at 568 nm ≈ 15) on a gold-covered glass slide and drying in a stream of nitrogen.

Quantitative analysis of the RA-FTIR data

Infrared external reflection spectroscopy has been widely used to investigate the structure and orientation of organic molecules in ultrathin films on metal surfaces (Allara and Nuzzo, 1985; Debe, 1982–1983, 1984; Mielczarski, 1993; Porter et al., 1987; Song et al., 1992). When the exciting light interacts with the molecular layers on the metallic support under nearly grazing angles of incidence, only the electric field normal to the support is active. In consequence, only the surface-normal components of the vibrational transition moments of the molecular layers will be sensed through the interaction with the resultant electric field perpendicular to the surface (Greenler, 1966). This is of particular interest for determination of the orientational distributions of the molecules in an anisotropic thin organic films, such as the polypeptide monolayers in the present investigation.

For the evaluation of the RA-FTIR spectra in terms of orientational order parameters of peptide molecules, we refer to Fig. 3. Shown is the laboratory-fixed rectangular x, y, z coordinate system, where the only active electrical field component of the incoming light (in the direction of the x axis) is E_z, perpendicular to the x-y surface of the substrate with the supported peptide monolayer. As will be shown in the Results, in the present work we have dealt exclusively with monolayers of helical polypeptides. In Fig. 3 an individual peptide helix is represented as a rodlike molecule with an instantaneous orientation characterized by the polar angles θ and φ of the principal helix axis H in the Cartesian coordinate system. Furthermore, the optical transition moment μ is indicated, which might correspond to either the amide I or the amide II mode of the peptides under investigation.

The ensemble of polypeptide helices in the anisotropic monolayer shows a certain distribution around the optical axis z, which can be described by the orientational order parameter S_h:

$$\langle P_2(z \cdot h)\rangle \equiv S_h = \int P_2(z \cdot h) f(\theta) \sin\theta \, d\theta \qquad (1)$$

Here, as well as in all following cases, the angular brackets indicate ensemble average. The probability that the angle between the director and the molecular axis has a value between θ and $\theta + d\theta$ can be written as $f(\theta)\sin\theta \, d\theta$, where $f(\theta)$ is the orientational distribution function of the helices and $P_2(z \cdot h)$ is the second Legendre polynomial,

$$P_2(z \cdot h) = \frac{1}{2}(3\cos^2\theta - 1) \qquad (2)$$

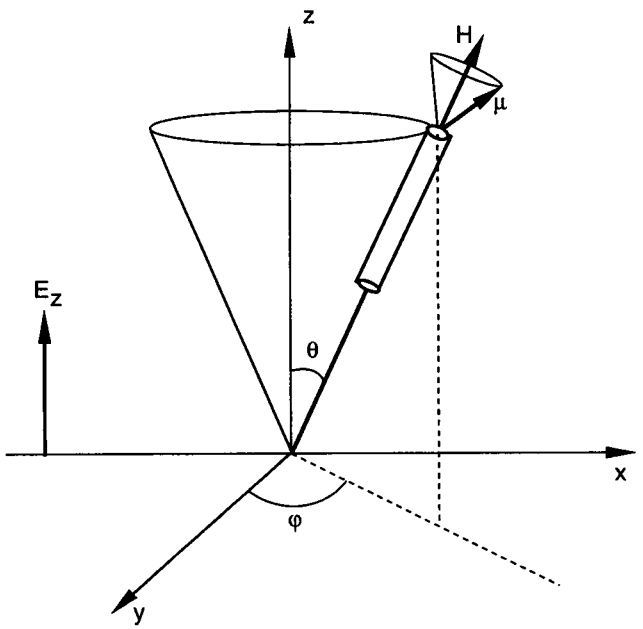

FIGURE 3 Schematic representation of an infrared external reflection experiment, used for the quantitative analysis of the RA-FTIR spectra in terms of molecular orientation. Shown is the laboratory-fixed rectangular x, y, z coordinate system and the only IR active electric field component of the incoming light E_z. An individual helical peptide molecule is represented as a cylinder with a main helix axis H and a transition dipole moment μ, corresponding to amide I or amide II mode. The instantaneous position of the peptide molecule is defined by the polar angles θ (between the main helix axis and the sample normal) and φ (between the projection of the main helix axis in the x-y plane and the y axis).

$(z \cdot h) = \cos\theta$ is the dot product of z, the unit vector along the z-axis, with h, the unit vector along the average helix axis H.

The intensity I of an RA absorption band is given by

$$I \propto \langle (z \cdot \mu)^2 \rangle \qquad (3)$$

By using spherical harmonics, the intensity of an absorption band can be simply expressed by molecular orientations in the general form

$$\langle (z \cdot \mu)^2 \rangle = \frac{1}{3}(2\langle P_2(z \cdot \mu)\rangle + 1) \qquad (4)$$

where, according to the addition theorem (Jackson, 1975), the following relation holds:

$$P_2(z \cdot \mu) = P_2(z \cdot h)P_2(h \cdot \mu) + \frac{1}{3}P_2^1(z \cdot h)P_2(h \cdot \mu)\cos\varphi + \frac{1}{12}P_2^2(z \cdot h)P_2^2(h \cdot \mu)\cos 2\varphi \qquad (5)$$

In the case of an uniaxial distribution for both μ around h and h around z, because of ensemble averaging in $\langle P_2(z \cdot \mu)\rangle$, the terms with $\langle\cos\varphi\rangle$ and $\langle\cos 2\varphi\rangle$ are zero, and

$$\langle (z \cdot \mu)^2 \rangle = \frac{1}{3}(2\langle P_2(z \cdot h)\rangle\langle P_2(h \cdot \mu)\rangle + 1) \qquad (6)$$

with

$$P_2(h \cdot \mu) = \frac{1}{2}[3(h \cdot \mu)^2 - 1] \qquad (7)$$

By using the orientational order parameters S_h and S_μ, Eq. 6 can be rewritten as

$$I \propto \langle (z \cdot \mu)^2 \rangle = \frac{1}{3}(2S_hS_\mu + 1) \qquad (8)$$

where S_μ, the orientational order parameter of the transition moment μ, is defined analogously to S_h in Eq. 1.

In this context, it is reasonable to compare the amide I and amide II transition modes, because it is known that the two transition moments are oriented approximately perpendicular to each other. The intensities $I_{(I)}$ of the amide I and $I_{(II)}$ of the amide II modes of the peptide monolayers on gold can be expressed by

$$I_{(I)} = C_I\frac{1}{3}(2S_hS_{\mu(I)} + 1) \qquad (9a)$$

and

$$I_{(II)} = C_{II}\frac{1}{3}(2S_hS_{\mu(II)} + 1) \qquad (9b)$$

where $S_{\mu(I)}$ and $S_{\mu(I)}$ are the orientational order parameters of the transition dipole moments of the amide I and amide II modes, respectively, and C_I and C_{II} are the corresponding proportionality constants. To compare the intensities of amide bands of different samples, it is reasonable to define relative intensities to avoid the explicit calculation of specific experimental parameters. The experimentally accessible and, in this context, relevant ratio $I_{(I)}/I_{(II)}$ is given by

$$\frac{I_{(I)}}{I_{(II)}} = C\frac{2S_hS_{\mu(I)} + 1}{2S_hS_{\mu(II)} + 1} \qquad (10a)$$

with $C = C_I/C_{II}$.

Obviously, if C, $S_{\mu(I)}$, and $S_{\mu(II)}$ are known, the ratio of the two intensities allows the determination of the molecular orientation of α-helices on gold. In principle, C might be determined by using a monolayer peptide film of no preferential molecular orientation of the helices, i.e., $S_h = 0$. However, such a situation is difficult to realize because of the inherent self-organizing tendency of the peptides under investigation. The orientational distributions of the amide I and amide II transition moments in α-helical polypeptides are not yet clearly determined. The reported literature values for the average orientation of the transition moment of the amide I mode with respect to the principal helix axis range from 17° to 40°, and the corresponding values for the amide II mode from 75° to 88° (Goormaghtigh et al., 1994a, and references therein). In principle it is possible to calculate the orientation of $\mu_{(I)}$ and $\mu_{(II)}$ in an ideal helix reasonably well, combining details of the three-dimensional structure and the normal-mode analysis of α-helices (Krimm and Reisdorf, 1994). Unfortunately, ideal α-helices do not exist in reality. Static structural distortions and conformational fluctuations within the polypeptide helices lead to deviations from the average α-helical structure in a sequence and positional dependence: the largest deviations are usually observed at the helix termini, as well as in flexible regions that are induced by kinks (Edholm et al., 1995; Vogel et al., 1988, 1993). Therefore, orientational distributions of transition moments with respect to an average or principal helix axis as described by S_μ are a better representation of the reality rather than fixed angles. To determine S_h for a particular polypeptide, the following strategy was applied. RA-FTIR measurements of two different polypeptide layers on gold were performed: one with the principal helix axis oriented perpendicular to the gold surface, the other parallel to it. By using these two reference spectra, together with the published values for the orientation of the amide transition moments, the range of possible values of C can accordingly be determined, in principle, from Eq. 10a.

As a first reference we used BR, a representative example of a membrane protein comprising seven transmembrane helical segments. According to electron diffraction studies of purple membranes, i.e., the natural membrane fragments containing well-defined, two-dimensionally ordered BR molecules (Grigorieff et al., 1996), the known high-resolution three-dimensional structure of BR defines the average orientation of the helices with respect to the membrane surface. A helical order parameter of $S_h = 0.83$ was calculated for such layers (Thiaudière et al., 1993). Numerous independent studies have proved that purple membranes can be spread in a functionally active form on solid supports, with the membrane planes preferentially aligned with the surface of the support (Blasie, 1994; Trissl and Gärtner, 1987). Actually, the system is further complicated by additional disorder in the protein layer, introduced by the nonideally flat surface of the support. This effect can be described by the so-called mosaic spread order parameter S_m of the membrane fragments around the normal of the support (Rothschild and Clark, 1979). Therefore, Eq. 10a must be extended by introducing S_m in the products of the order parameters:

$$\frac{I_{(I)}}{I_{(II)}} = C\frac{2S_hS_{\mu(I)}S_m + 1}{2S_hS_{\mu(II)}S_m + 1} \qquad (10b)$$

For practical purposes, we define an apparent transition moment order parameter $S'_\mu = S_\mu S_m$ as the product of the intrinsic transition moment order parameter S_μ and the mosaic spread order parameter S_m.

In the present investigation we do not use explicit S_m values, but rather the corresponding S'_μ values. As the solid supports used for all peptide layers were identical, we assume identical S_m values in all cases.

As a second reference, that of an in-plane oriented polypeptide α-helix, we have chosen the His-peptide. This peptide was designed as an ideal amphipathic, straight helix (see Fig. 2). It will be shown in the Results that at the air/water interface the peptide helix is oriented in the plane of the interface, and preserves its molecular structure and orientation after both LB transfer and SA on a solid support. Its monolayers are therefore characterized by $S_h = -0.5$.

Polarization modulation infrared reflection absorption spectroscopy

Peptide monolayers at different stages of monolayer compression were studied directly at the air/water interface by PM-IRRAS. The differential reflectivity measurements offer a unique possibility to study the secondary structure and orientation of the peptides at the air/water interface during the whole compression/expansion cycle in situ. Essentially, PM-IRRAS combines FTIR reflection spectroscopy with fast polarization modulation of the incident beam between parallel (p) and perpendicular (s) polarization. Two-channel electronic and mathematical processing of the detected signal makes it possible to obtain the differential reflectivity spectrum $\Delta R/R = (R_p - R_s)/(R_p + R_s)$ (Blaudez et al., 1996). The spectra were recorded at the University of Bordeaux with a Nicolet 740 spectrometer with a HgCdTe detector by coaddition of 300 scans at a resolution of 4 cm^{-1}, Happ-Genzel apodization function, and a level of zero filling equal to 1. The PM-IRRAS set-up and experimental procedure have been reported in detail elsewhere (Blaudez et al., 1994). To eliminate the contribution of the water absorbance and the second Bessel function, the spectra obtained from the peptide monolayers were divided by those of a pure water surface. The surface selection rule in PM-IRRAS spectroscopy under the particular experimental conditions (angle of incidence 75° and water as a substrate) determines the position of the absorption bands relative to the baseline: positive absorption occurs for transition moments preferentially in the plane of the substrate, whereas negative absorption corresponds to transition moments oriented perpendicular to the substrate surface (Blaudez et al., 1994).

Sample preparation

For the formation of Langmuir monolayers in the PM-IRRAS experiments, a methanol/dichloromethane (1:9) peptide solution was applied to the water surface at a surface pressure of 0 mN/m. The monolayers were compressed to the desired surface pressure by means of a mobile barrier. The PM-IRRAS spectra of the layers were measured 15 min after the surface pressure reached the predefined value. Spectra of the His-peptide were measured on a subphase containing 0.025 M glycine/NaOH buffer (pH 9) or 0.025 M citric acid/Na_2HPO_4 buffer (pH 3).

Circular dichroism

CD experiments were performed on an AVIV model 62 DS circular dichroism spectrometer (AVIV, Lakewood, NJ). Spectra were recorded between 192 and 250 nm (step resolution of 2 nm) at 20°C with a quartz cuvette of 0.1-mm path length. Each experiment was repeated four times. Reference samples of the solvent (methanol/dichloromethane = 1:9) were routinely recorded and subtracted from the original spectra. Because the dichroic behavior of peptides in the far UV is dominated by their secondary structure, the CD spectra were used to determine the average conformation of the peptides in organic solution. The molar ellipticity at 222 nm, Θ_{222}, was used to estimate the helical content of the two peptides; it was shown to be, to a good approximation, proportional to the α-helix content in polypeptides, with a value of -3×10^4 deg $dmol^{-1}$ cm^2 corresponding to 100% helical conformation (Chen et al., 1974).

Molecular dynamics

The MD simulation of the peptides was performed with the program CHARMM (Brooks et al., 1983), with the parameter set Charmm 22. As initial coordinates, we chose those of an ideal helix. All atoms of the polypeptides were treated explicitly. The MD calculations were performed in vacuum with 1-fs time steps by using the Langevin algorithm and taking into account an average friction caused by the molecular motions of the polypeptides relative to their surroundings (Brooks et al., 1985). A friction coefficient of 5 ps^{-1} and a dielectric constant of 1.758 corresponding to those of methanol were used. The total simulation time spanned 1 ns.

RESULTS

Secondary structure of the peptides in the solid state and in solution

The ultimate goal of the present work is the formation of monolayers of helical peptides at interfaces. We therefore investigated first whether the considered peptides are able to adopt a helical conformation in helix-inducing, nonpolar solvents. We believe that a stable helical conformation in solution is a prerequisite and a good indication that a peptide will also, in turn, be helical at interfaces. Second, the peptide conformation in the bulk solid state was studied, as it should compare well to the situation in which the peptides are immobilized as a densely packed monolayer at interfaces.

Fig. 4 shows the CD spectra of the two peptides in organic solution. The Θ_{222} values of -2×10^4 and -2.7×10^4 deg dmol^{-1} cm^2 for the A- and the His-peptide, respectively, correspond to a helix content of 75% and 90%. The protonation of the histidine and lysine residues in the His-peptide did not change the helix content in solution (spectrum not shown).

The amide I and amide II regions of FTIR transmission spectra of the two peptides in organic solution were quite similar (Tables 1 and 2). In Fig. 5 only the spectra of the solid peptides are shown.

In the case of the His-peptide, maximum intensities were observed at 1658 ± 1 cm^{-1} for the amide I region and at 1544 ± 1 cm^{-1} for the amide II region (Fig. 5 *A*). The amide I region was decomposed into three individual bands (1638, 1658, 1680 cm^{-1}), and the amide II region into two bands (1524, 1544 cm^{-1}). According to normal-mode analysis and numerous spectra of polypeptides of known structures (Krimm and Reisdorf, 1994), the FTIR spectra strongly support the CD results of a predominantly helical structure of the peptide. NMR spectroscopic analysis has also shown a largely helical conformation of the peptide (Bechinger, 1996).

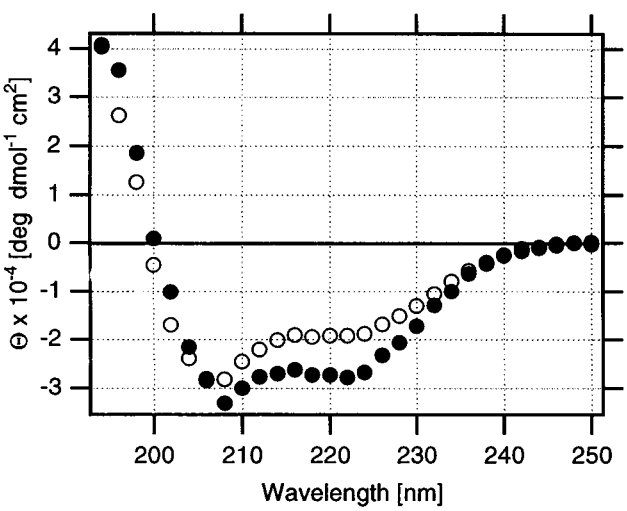

FIGURE 4 CD spectra of the A-peptide (○) and His-peptide (●) in methanol/dichloromethane (1:9) solution. The peptide concentrations were 4.3×10^{-4} M (A-peptide) and 2.1×10^{-4} M (His-peptide), the temperature 20°C, and the optical path length 0.1 mm.

TABLE 1 Peak positions in the amide I and amide II regions in FTIR spectra of His-peptide and A-peptide under different sample conditions

	His-peptide		A-peptide	
Sample	amide I (cm^{-1})	amide II (cm^{-1})	amide I (cm^{-1})	amide II (cm^{-1})
Solution	1658	1551	1660	1545
Solid state	1658	1544	1660	1538
Air/water interface	1658	1545	1660	1542
On Ge: LB transfer*	1658	1543	1660	1541
On Au: LB transfer*	1661	1546	1663	1542
SA monolayer	1663	1547	1675	1542

*The LB transfers were performed at a surface pressure of 8 mN/m.

In the A-peptide spectra, the amide I band was centered at 1660 ± 1 cm^{-1}, and the amide II at 1538 ± 1 cm^{-1} (Fig. 5 *B*). Three absorbance bands were resolved by curve fitting in the amide I region (at 1640, 1662, and 1688 cm^{-1}), and two in the amide II region (at 1517 and 1538 cm^{-1}). Regular α-helical structures typically give rise to amide I bands at 1650–1658 cm^{-1} (Surewicz et al., 1993). The shift to higher wavenumbers in the case of the A-peptide might indicate the presence of distorted and/or 3_{10}-helical structures (Haris and Chapman, 1988, 1995; Krimm and Reisdorf, 1994; Rothschild and Clark, 1979). Furthermore, the major amide I band is considerably broader than in the case of the His-peptide, indicating a larger distribution of slightly different helical structures. This is quite reasonable, because the pseudo-proline residue induces a kink in the central part of the A-peptide (see Fig. 2). It has been shown that proline-induced kinks represent a flexible element in helical polypeptides (Vogel et al., 1993).

For both peptides, the major amide I transition was accompanied by two weaker bands, one at lower and one at higher wavenumbers. Although vibrational transitions of nonhelical peptide structures appear in these spectral regions, the observed bands can also stem from helical structures. Normal-mode analysis has shown that purely helical (α-helical, 3_{10}) polypeptides indeed have considerable spectral contribution from both sides of the major amide I band (Krimm and Reisdorf, 1994; Torii and Tasumi, 1996).

In summary, IR and CD spectroscopy has shown that both the A- and the His-peptides adopt a predominantly helical conformation, as expected from their amino acid sequences.

Peptide monolayers at the air/water interface

Langmuir isotherms

When spread at the air/water interface, both the A- and the His-peptide formed stable monolayers. Fig. 6 shows the surface pressure/area (π/A) isotherms of the two peptide monolayers. The behavior of the monolayers was independent of the temperature in the range of 15–30°C. In a

TABLE 2 Position of the individual bands resolved in the amide I and amide II regions of His-peptide, A-peptide, and BR FTIR spectra obtained under different sample conditions

	His-peptide*			A-peptide*			BR*
Spectral region	Solid bulk sample	LB monolayer on gold	SA monolayer on gold	Solid bulk sample	LB monolayer on gold	SA monolayer on gold	Oriented multilayers on gold
amide I (cm^{-1})	1638	1641	1641	1640	1646	1649	1623
	1658#	1661#(‖)	1662#(‖)	1662#	1664#(‖)	1663(‖)	1649
		1673(⊥)	1673(⊥)		1676(⊥)	1676#(⊥)	1668#(⊥)
	1680	1687	1687	1688	1686	1687	1684
amide II (cm^{-1})	1524	1531	1530	1517	1528	1516	1518
	1544	1548	1547	1538	1543	1543	1544

*Data from the spectra shown in Figs. 5, 8, and 9. Indicated are the parallel (‖) and the perpendicular (⊥) components of the amide I transition dipole moment with respect to the main helix axis, giving rise to the particular bands.
#Major band.

compression/expansion cycle, the isotherms of both peptides were reversible between 0 and 30 mN/m. Further compression of the monolayers is not reported, because due to the extremely high layer viscosity, the Wilhelmy plate system was no more functional above 30 mN/m. Similar behavior has been observed with other peptides, e.g., TASP-melittin (Meseth, 1996), M13 phage coat and procoat proteins (M. Boncheva, unpublished results).

The four histidine and two lysine amino acid residues in the His-peptide can be protonated and deprotonated by changing the pH in the surrounding aqueous phase, making it possible to reversibly switch the molecular electrical charges on and off. The influence of surface charges on the molecular packing in His-peptide monolayers was investigated by recording the corresponding π/A isotherms at pH 3 (six positive charges per molecule) and pH 9 (two positive charges at the C-terminus of each molecule), as shown in Fig. 6 *A*. The molecular area of the peptide at 30 mN/m increased by 0.56 nm^2 when the pH of the subphase was changed from 9 to 3, because of increased repulsive electrostatic interactions.

The pressure/area isotherms in Fig. 6 gave the first indication of the molecular orientation of the peptides at this interface. In the most densely packed monolayers (at a surface pressure of 30 mN/m), the molecular areas of the two peptides were 3.00 nm^2 for the A-peptide and 3.75 and 4.30 nm^2 for the His-peptide on a subphase of pH 9 and 3, respectively. By comparing these experimental values with the molecular dimensions of the helices calculated by molecular dynamics simulation (Table 5), it is possible to estimate the helix orientation on the water surface. The experimental data from the Langmuir isotherms indicate a preferential parallel orientation of the peptide helices at the water surface.

To obtain additional information about the peptide monolayers, the van der Waals equation of state for two-dimensional systems was used to describe the low-pressure region of the isotherms:

$$\pi = \frac{k_B T}{A_m - A_e} - \frac{a}{A_m^2} + c \qquad (11)$$

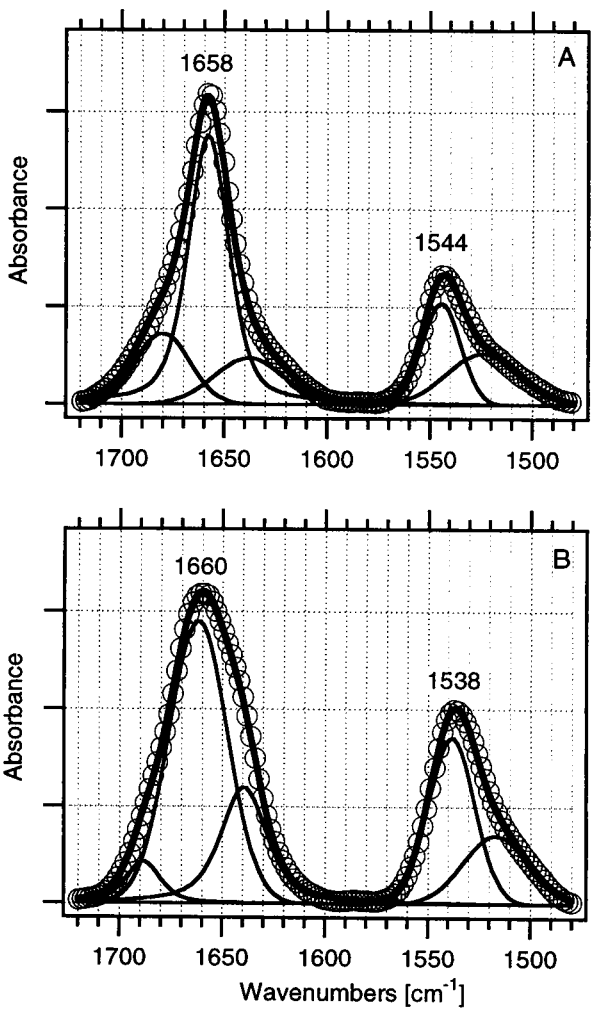

FIGURE 5 Transmission FTIR spectra of the His-peptide (*A*) and the A-peptide (*B*) as bulk solid samples on CaF_2 windows. The spectra are normalized for the amide I band intensities. Shown are the best-fitted individual bands (*thin solid lines*), their sum (*thick solid line*), and the experimental points (○). Indicated are the wavenumbers of the maximum intensities in the amide I and amide II regions.

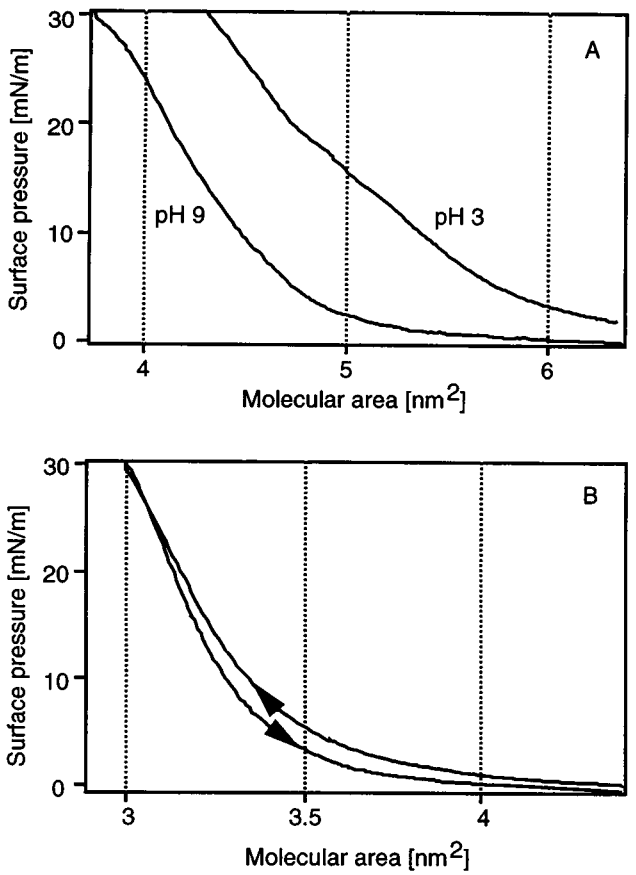

FIGURE 6 Surface-pressure/area isotherms of monolayers of His-peptide (*A*) and A-peptide (*B*). The temperature was 22 ± 2°C and the compression speed 0.05 nm^2 $molecule^{-1}$ min^{-1}. (*A*) Isotherms of His-peptide monolayer on aqueous subphase of pH 9 and 3 (for details, see Materials and Methods). (*B*) The arrows indicate compression or expansion of the monolayer spread on deionized water.

Here π is the surface pressure of the monolayer, A_e is the excluded area occupied by the peptide, by which the total area A_m in which the peptide can move freely is reduced, the parameter a accounts for the repulsive molecular interactions in the monolayer, and c is a correction factor to compensate for errors in the offset of the pressure measurements (Cevc and Marsh, 1987). The fit was reasonable up to 10 mN/m, yielding a value for A_e of 3.09 nm^2 for the A-peptide, and 4.23 and 5.14 nm^2 for the His-peptide on subphase pH of 9 and 3, respectively. Interestingly, the A_e value and the molecular area of the A-peptide at 30 mN/m are nearly identical, whereas in the case of the His-peptide, the A_e values are considerably higher than the corresponding molecular areas in the fully compressed state. Apparently, the electrostatic repulsion plays a more important role at low π. A higher compressibility of the His-peptide monolayers (7.3×10^{-3} m/mN and 8.89×10^{-3} m/mN for monolayers spread on subphases of pH 9 and 3, respectively) leads to a larger relative area reduction as compared to A-peptide monolayers (4.56×10^{-3} m/mN) (values at 20 mN/m). A comparable monolayer compressibility of $\sim 10^{-2}$ m/mN at 30 mN/m has been reported for other synthetic polypeptides (Fukushima et al., 1979).

No phase separation was observed in the peptide monolayers, either in the pressure/area isotherms or under the Brewster angle microscope in the studied surface pressure range. Although this indicates a homogeneous layer, the formation of smaller domains cannot be excluded, because the lateral resolution of the microscope was 2 μm.

PM-IRRAS measurements

The PM-IRRAS peptide spectra at the air/water interface (Fig. 7) were very similar to those in bulk solid state, and in solution. The amide I bands were centered at 1660 cm^{-1} for the A-peptide and 1658 cm^{-1} for the His-peptide, indicating the preservation of the helical conformation at the water surface. The His-peptide spectra were not modified upon changing the subphase pH from 9 to 3 (spectrum not shown). The amide I and amide II peak intensities increased continuously with the surface pressure over the 0–30 mN/m compression range. Although for both peptides the width of the amide I band decreased with increasing surface pressure in the range of 0–30 mN/m, the amide I band was always broader for the A-peptide than for the His-peptide, as in the transmission and the RA-FTIR spectra.

Under the present experimental conditions (angle of incidence of 75°), the surface selection rule for dielectric substrates predicts that transition moments lying on the average in the surface plane give rise to a positive absorption band; a negative absorption band is an indication of transition moments with an average orientation perpendicular to the surface (Blaudez et al., 1994). In the whole compression range, both peptides exhibited positive amide I and II bands, with the latter being considerably weaker. Cornut et al. (1996) have calculated PM-IRRAS spectra of peptide helices with different orientations at the water surface. According to these simulations, the spectra in Fig. 7

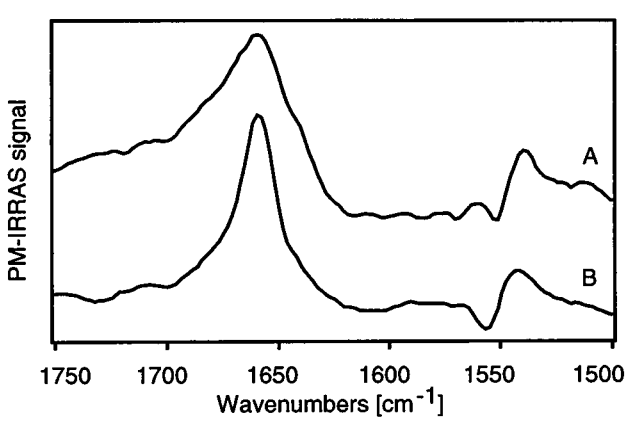

FIGURE 7 In situ PM-IRRAS spectra of A-peptide (*A*) and His-peptide (*B*) monolayers compressed to a surface pressure of 30 mN/m. The subphase was deionized water (*A*) or 0.025 M glycine/NaOH buffer, pH 9 (*B*). The spectra are normalized for the amide I band intensities.

indicate that the peptide helices are preferentially oriented parallel to the air/water interface.

Peptide monolayers on gold by RA-FTIR

Fig. 8 shows representative examples of RA-FTIR spectra of monomolecular films of the two peptides formed by LB transfer and self-assembly. In all cases, the RA-FTIR spectra differ from those in solution, either in wavenumbers or in relative intensities of the amide I and amide II bands. Table 2 summarizes the wavenumbers of the individual bands into which the amide I and amide II regions of the monolayers and solid bulk spectra were decomposed. For both peptides, the same number of bands was resolved independently of the layer formation method. In the spectra of A-peptide monolayers, all bands changed in wavenumber and relative intensity; in the spectrum of LB transferred monolayer, the major amide I band is at 1664 cm^{-1}, and in the case of self-assembled monolayer, at 1676 cm^{-1}. Compared to the transmission spectrum of the solid sample, this corresponds to a shift toward a higher wavenumber of 2 cm^{-1} for the LB-transferred monolayer, and of 14 cm^{-1} in the self-assembled monolayer. In the case of the His-peptide monolayers, the resolved individual bands remained with the same relative intensity independently of the layer formation method. The amide I maximum in LB-transferred monolayers was shifted by 3 cm^{-1}, and in self-assembled monolayers by 4 cm^{-1} toward higher wavenumbers as compared to the transmission spectrum. Obviously, the first question to arise is whether these spectral differences are induced by structural changes of the polypeptides in contact with gold surfaces, reorientation of the molecules at the gold surface, or the particular sampling technique.

To determine the conformation of the peptides in contact with the gold surface by an independent method, we are currently investigating the peptide secondary structure by ATR-FTIR experiments, using germanium supports covered by an ultrathin gold film. In this experimental config-

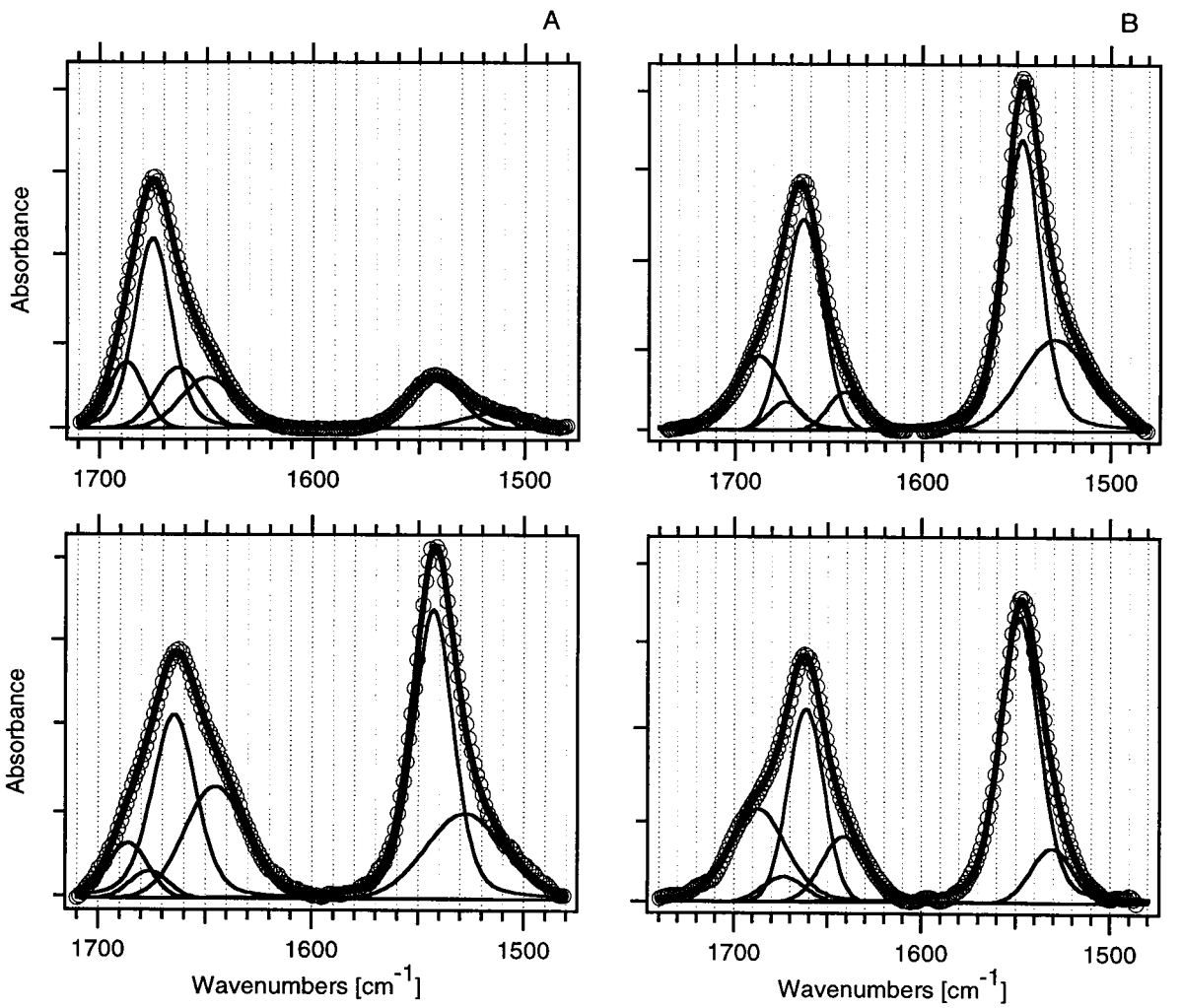

FIGURE 8 RA-FTIR spectra. (*A*) A-peptide monolayer. (*B*) His-peptide monolayer. The peptide monolayers were formed by self-assembly (*upper row*) or LB transfer at a surface pressure of 8 mN/m (*bottom row*). Shown are the best-fitted individual bands in the amide I and amide II regions (*thin solid lines*), their sum (*thick solid line*), and the experimental points (○). The spectra are normalized for the amide I band intensities.

uration, the molecules in contact with gold are sensed as in a conventional ATR spectroscopy, thus avoiding spectral changes as in the RA-FTIR technique. The peptides' secondary structure studied in LB-transferred monolayers on conventional germanium supports was found to be identical to the one in solution or in the solid state (Table 1). Our preliminary ATR-FTIR experiments with peptide monolayers self-assembled on gold do not show any significant differences in the spectra of LB transferred and self-assembled peptide monolayers compared to their respective spectra in solution (manuscript in preparation), demonstrating that the peptides preserve their helical conformation at the gold/air interface. Therefore, the differences in the peptides' RA-FTIR spectra compared to conventional FTIR spectra do not result from conformational changes of the peptides at this interface.

It is known from many investigations that RA-FTIR spectra of thin films on metal supports can differ considerably in frequency, intensity, and lineshape from the corresponding spectra in solution (Yen and Wong, 1989). This variation can be explained by the presence of surface modes corresponding to the transverse optical (TO) and longitudinal optical (LO) excitations of the thin film and by the optical properties of the substrate. The TO band appears near the oscillator frequency of bulk samples, whereas the LO band is shifted to higher frequencies by an amount roughly proportional to the absorption strength (Lyddane et al., 1941).

Furthermore, in the particular case of helical polypeptides, two different components of the LO amide I mode can be excited (Cantor and Schimmel, 1980; Fringeli and Günthard, 1981; Goormaghtigh et al., 1994a): one with a strong transition dipole moment component, μ_z, along the main helix axis, and the other with weaker transition dipole moment components, μ_x and μ_y, perpendicular to the first one (Fig. 3). Therefore, a reorientation of the peptide helices with respect to the plane of the metal support would result in excitation of the amide I mode at a different wavenumber compared to the one observed in solution. When the helices are oriented with their main axis in the plane of the interface, the $\mu_x - \mu_y$ components will be preferentially excited; as it is a weak transition, its wavenumber should be close to the one observed in the bulk spectrum. Analogously, when the helices are oriented perpendicular to the interface, the μ_z component is excited. As the dipole moment along the z-axis is much stronger than the ones in the x-y plane, a stronger TO/LO splitting is expected in this case, and the amide I band is expected to shift 8–10 cm^{-1} to higher wavenumbers (Allara et al., 1978).

The considerations presented above deliver an explanation for the differences between the transmission and RA-FTIR spectra of the peptides. In the case of the His-peptide, the major amide I band observed in the transmission spectrum is centered at 1658 cm^{-1}. According to the existence of the surface modes described above, this band is shifted to the higher wavenumbers in the RA-FTIR spectra, and is furthermore split in two: one part corresponding to excitation of the $\mu_x - \mu_y$ components (1661–1662 cm^{-1}), and the other to the μ_z component (1673 cm^{-1}) of the transition dipole moment (Fig. 8 and Table 2). The fact that the wavenumber of the major amide I band in RA-FTIR and transmission spectra are similar (shift of 3 cm^{-1} in the spectrum of LB transferred and 4 cm^{-1} in self-assembled monolayers) indicates that in both cases the $\mu_x - \mu_y$ components of the dipole moment are preferentially excited, i.e., the helices are oriented parallel to the plane of the support. Our SPR measurements (see below) fully confirmed this conclusion.

In the case of the A-peptide, the major amide I band appears at 1662 cm^{-1} in the transmission spectrum of bulk solid samples, at 1664 cm^{-1} in the RA-FTIR spectrum of LB transferred monolayers, and at 1676 cm^{-1} in the RA-FTIR spectrum of self-assembled monolayer (Fig. 8 and Table 2). The shift between the transmission and the RA-FTIR spectrum of the LB-transferred monolayer can be explained by the preferential excitation of the surface $\mu_x - \mu_y$ components of the dipole moment; thus an orientation of the helices parallel to the surface is deduced. The observed shift of 14 cm^{-1} in the spectrum of the self-assembled monolayer could indicate only a reorientation of the peptide helix. As the μ_z component of the dipole moment is considerably stronger than the $\mu_x - \mu_y$ components, its excitation would lead to a proportionally big shift in the observed amide I wavenumber. Therefore, a molecular orientation close to perpendicular to the surface is concluded for the A-peptide self-assembled monolayer.

As described in Materials and Methods, the evaluation of the orientational distribution of the A-peptide helices was based on two reference systems: BR as an example of helices oriented perpendicular to the interface, and the His-peptide monolayer as an example of helices oriented parallel to the gold surface. Figs. 8 and 9 show the RA-FTIR spectra of the peptides immobilized on gold by different immobilization procedures (LB transfer or SA) and the reference spectrum of an oriented monolayer of purple membranes. The comparison of the A-peptide spectra with those of the two reference systems reveal two major points: 1) The spectrum of the LB-transferred monolayer, with respect to position of the major amide I band and its relative intensity to the major amide II band, is close to the spectra of the His-peptide monolayers. The major amide I band appears at 1664 cm^{-1}, corresponding well to the one in the His-peptide spectra (1661 cm^{-1}). In all three spectra, this band is of considerably lower intensity than the major amide II band. 2) On the other hand, the spectrum of the self-assembled A-peptide monolayer is very similar to the spectrum of BR. In both cases, the major amide I band is of higher intensity than the major amide II band, and appears at comparable wavenumbers.

The ratios between the major amide I/amide II bands were calculated by using the integrated areas of the bands around 1668–1676 cm^{-1} and 1543–1548 cm^{-1}, respectively (Table 3). These particular amide I and amide II bands were chosen because they correspond to the prefer-

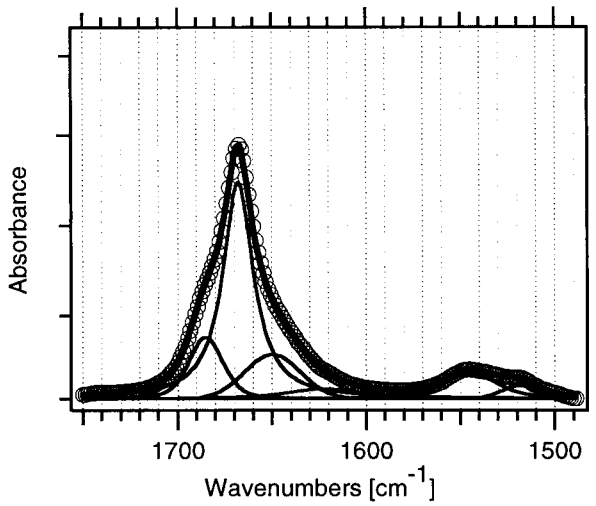

FIGURE 9 RA-FTIR spectrum of BR in purple membranes on a planar gold surface. Shown are the best-fitted individual bands in the amide I and amide II regions (*thin solid lines*), their sum (*thick solid line*), and the experimental points (○). The spectrum is normalized for the amide I band intensities of the spectra in Fig. 8.

ential parallel and perpendicular transition moments, as can be already seen qualitatively from their corresponding intensity ratios in the different monolayer spectra.

The unchanged amide I wavenumber and intensity ratio $I_{(I)}/I_{(II)}$ show that the orientation of the His-peptide in the self-assembled monolayer did not differ from the one in the LB-transferred monolayers of both the His- and the A-peptide. To quantify S_h of the A-peptide in self-assembled monolayers, it is necessary to know the values of C, $S'_{\mu(I)}$, and $S'_{\mu(II)}$ in Eq. 10b. As in this equation, we have three unknowns but only two calibration spectra (that of BR with $S_h = 0.83$ and $I_{(I)}/I_{(II)} = 5.73$, and that of the LB-transferred layer of the His-peptide with $S_h = -0.5$ and $I_{(I)}/I_{(II)} = 0.08$; see Table 3), we used the published values for the orientation of the amide transition moments ($S_{\mu(I)} = 0.86$ to 0.73 and $S_{\mu(II)} = -0.4$ to -0.5) to limit the possible values of the constant C to 0.798–0.444. By using this range of C values, the orientational distribution of the average helices in the A-peptide self-assembled monolayers is restricted to $S_h = 0.63 \pm 0.063$, assuming $S_m = 1$. S_h defines the orientational distribution of the average helix axes of the A-peptides around the normal to the support. Unfortunately, according to Eq. 1, the orientational distribution function $f(\theta)$ is not known explicitly. If we assume, however, for later comparison with the SPR data a uniform orientation of the helices with a fixed tilt angle θ of the principal molecular axis, a value of $S_h = 0.63 \pm 0.063$ corresponds to $\theta = 30 \pm 3°$. Using this tilt angle and the molecular dimensions obtained from the molecular dynamics simulation (Fig. 2), an average thickness of 2.6 nm was calculated for the self-assembled A-peptide monolayers. Nevertheless, we want to point out that these formal evaluations do not prove an actual uniform tilt angle. A more realistic interpretation of S_h, in our opinion, is a distribution of orientations of the helices.

TABLE 3 Intensity ratios $I_{(I)}/I_{(II)}$ between the amide I and amide II bands of RA-FTIR spectra of BR, His- and A-peptide layers on gold

Layer	$I_{(I)}/I_{(II)}$
BR	$I_{(1668)}/I_{(1544)} = 5.73$
His-peptide	
LB transfer	$I_{(1673)}/I_{(1548)} = 0.08$
SA monolayer	$I_{(1673)}/I_{(1547)} = 0.08$
A-peptide	
LB transfer	$I_{(1676)}/I_{(1543)} = 0.08$
SA monolayer	$I_{(1676)}/I_{(1543)} = 2.85$

Peptide monolayers on gold by SPR

Table 4 summarizes the results of the SPR measurements performed with self-assembled and LB-transferred peptide monolayers on gold.

In the case of the His-peptide, a value of $d = 0.8$ nm was obtained for the thickness of a self-assembled monolayer. Together with the calculated molecular area of $A_{SPR} = 4.06$ nm^2, this result indicates that the helices are preferentially oriented parallel to the surface. The LB-transferred monolayers showed slightly increased thickness and concomitant decreased mean molecular areas; this finding could be interpreted as a slight tilt of the peptide helices toward the solid support, induced by the high lateral compression of the peptide layer on the water surface.

The SPR results for the A-peptide monolayers in Table 4 are in complete agreement with the conclusions drawn from the FTIR experiments, demonstrating a predominantly parallel orientation in LB-transferred and perpendicular orientation with respect to the support in self-assembled monolayers. The mean layer thickness of 2.12 nm in the self-assembled A-peptide monolayers, as measured by SPR, corresponds well to the one calculated from our RA-FTIR measurements (2.6 nm). The difference of 15% in the thickness as measured by the two methods can easily be explained by their different sensitivities to the presence of impurities adsorbed on the gold surface.

The refractive index of the peptide monolayers was obtained by fitting the experimental reflectance versus angle of incidence curves with the Fresnel equations, using the

TABLE 4 SPR experiments: resonance angle shift $\Delta\theta^{spr}$, mean molecular area A_{SPR}, and monolayer thickness d of the His- and A-peptide monolayers immobilized on gold by LB transfer and self-assembly

Experiment	$\Delta\theta^{spr}$ (°)	A_{SPR} (nm^2)	d (nm)
His-peptide			
LB transfer*	0.34	3.05	1.06
SA monolayer	0.30	4.06	0.8
A-peptide			
LB transfer#	0.34	2.36	1.07
SA monolayer	0.68	1.19	2.12

*The LB transfer was performed at a surface pressure of 28 mN/m.
#The LB transfer was performed at a surface pressure of 30 mN/m.

calculated monolayer thickness. The considerably high value of 1.59 indicates a dense packing in the peptide layers.

DISCUSSION

The present results have demonstrated that stable helical peptide monolayers can be formed at the surface of water and various solid supports. Most importantly, the molecular orientation of the hydrophobic helices in the layer can be controlled by choosing a particular procedure for the layer formation. This opens, for the first time, the possibility of controlling the structure of protein layers at interfaces for various applications.

Here we will focus on the following major results of our work, which were of importance in reaching the above conclusion: first, the feasibility of pure peptide layer formation at different interfaces by using synthetic polypeptides; second, the parameters that determine the molecular orientation in such monolayers; third, the method we propose for calculation of the helical order parameter from RA-FTIR data.

1. In the present study we investigated the formation and structural properties of peptide assemblies at different interfaces, using either amphipathic or hydrophobic polypeptide helices. The stable helix structure of both polypeptides in organic solution and bulk solids was found to be unchanged in monolayers at the air/water and air/solid interfaces, in contrast to the often observed phenomenon that water-soluble proteins and polypeptides denature at the air/water interface or upon contact with the support (Jakobsen and Wasacz, 1987; Jakobsen et al., 1985; MacRitchie, 1987; Smith and Clark, 1992). To our knowledge, RA-FTIR measurements were used for the first time to deliver direct experimental evidence for the molecular conformation of pure peptide monolayers. Synthetic polypeptides can exist in different structural conformations, e.g., α-helices, β-strands, or nonregular states, each with distinct mechanical, optical, electrical, magnetic, and biological properties. The present study shows the possibility of constructing immobilized peptide monolayers with predefined macroscopic properties and molecular structure by choosing the proper amino acid sequence of the polypeptides composing the layer.

2. The molecular orientation of the peptides in interfacial monolayers was investigated by different techniques: at the water surface, by π/A isotherms in a Langmuir film balance as well as by FTIR spectroscopy; in the case of supported peptide layers, by a combination of FTIR and SPR measurements. π/A isotherms and SPR measurements deliver mean molecular areas. These, in turn, can be used to estimate the molecular orientations in the corresponding peptide films when compared with molecular models of the peptide helices. Table 5 summarizes the molecular areas of the His-peptide and the A-peptide in LB-transferred and self-assembled monolayers as estimated from different molecular models and experiments. Such information is complementary to FTIR measurements, which gave direct information on the orientational distribution of the α-helical polypeptides at the different interfaces. It is interesting to compare the different molecular areas listed in Table 5, because they give an idea of the validity and strength of the different models.

TABLE 5 Molecular areas of the His-peptide and the A-peptide in LB-transferred and self-assembled monolayers as estimated from molecular models and experiments

Model/experiment	His-peptide (nm^2)	A-peptide (nm^2)
A_{MD}*#		
Perpendicular	1.13	0.95
Parallel	4.44	3.50
A_S§		
Perpendicular##	0.87	0.79
Parallel*§§	3.90	3.20
Parallel¶¶	3.46	2.83
A_{vdW}¶	4.23|||	3.09
A_i||	3.75|||	3.00
A_{SPR}**		
LB transfer	3.05	2.36
SA monolayer	4.06	1.19

*Calculated assuming a cylindrical shape for the peptide helices.
#Calculated as a molecular projection using the dimensions obtained from MD (see Fig. 2).
§Calculated as the area of a single peptide molecule, using a molecular density $\rho = 1.37$ g/cm^3 (Gennis, 1989), the mass of the peptides m, and the helix length ℓ obtained from MD (see Fig. 2).
¶Calculated as $A_{vdW} = A_e$ in Eq. 11.
||Area at a surface pressure of 30 mN/m (see Fig. 6).
**Data from Table 4.
##Calculated as $A_S = m/(\ell\rho)$.
§§Calculated as $A_S = 2\,(\ell m/\pi\rho)^{1/2}$.
¶¶Calculated assuming a square molecular projection, i.e., $A_S = (\ell m/\rho)^{1/2}$.
|||Data for His-peptide monolayers spread on subphase of pH 9.

We start our consideration with the molecular models obtained from MD. The computer simulations have revealed that the two polypeptides remain stable α-helices, in agreement with our spectroscopic experiments. From the calculated α-helical structures in Fig. 2, it is possible to estimate the projection area A_{MD} of a single polypeptide in a parallel ($\parallel$) or perpendicular ($\perp$) surface orientation. The corresponding values, assuming a cylindrical shape of a polypeptide helix, are 4.44 ($\parallel$) and 1.13 ($\perp$) nm^2 for the His-peptide, and 3.50 ($\parallel$) and 0.95 ($\perp$) nm^2 (calculated as a projection of the helical segment 1–10) for the A-peptide, respectively. Because of interdigitization of side chains of neighboring molecules, however, the molecular areas in a peptide monolayer might be smaller than those of the individual molecules. More realistic mean molecular areas in condensed monolayers can be estimated by using the partial specific volumes of proteins ($1/\bar{V} = 1.37$ g/cm^3) (Gennis, 1989) and the length of a stable α-helix as obtained from the MD. The corresponding molecular areas (A_S in Table 5) are 10–20% lower than the values estimated for single molecules. It is interesting to note that the experimentally determined mean molecular areas A_i of compressed His- and

A-peptides at the water surface are between those estimated for parallel orientation of peptides of circular and square cross sections. Obviously, a cylindrical structure is an oversimplification, because the peptide side chains are flexible enough to reorient under compression toward a more square cross section of the polypeptide helix. The same also holds for A-peptides as described by a two-dimensional van der Waals equation (Eq. 11), whereas the His-peptide under the same conditions shows a distinctly larger area A_{vdW}. This difference reflects the influence of electrical charges in the case of the His-peptide. Taken together, both the hydrophobic A-peptide and the amphiphilic His-peptide adopt a parallel orientation on the water surface.

The mean molecular areas A_{SPR} of LB-transferred peptide films are ~20% lower than those estimated before for the parallel surface orientation (A_i). In view of the quite different experimental technique, we believe that this difference is still in agreement with a parallel surface orientation in the LB-transferred monolayers. In this context, one should note also that the accuracy of the mean molecular area determination on the Langmuir film balance under our experimental conditions is not better than 20%. Nevertheless, the values of A_{SPR} could also indicate a slight deviation from an ideally flat orientation of the α-helices in LB-transferred monolayers. The situation, however, changes drastically when self-assembled monolayers of His- and A-peptide are compared. Whereas the His-peptides are still oriented parallel to the surface, the A-peptide areas clearly indicate a perpendicular helix orientation.

Several parameters were found to play an important role for the molecular orientation in the studied polypeptide monolayers: 1) the type of interface, 2) the amino acid sequence, 3) the specific peptide interactions with the support, and 4) the method of layer formation.

To illustrate the influence of the interface on the layer properties, we compared the molecular orientation in A-peptide monolayers in the same surface pressure range (0–30 mN/m) on water and after LB transfer to hydrophilic gold surfaces. At the air/water interface, both the hydrophobic and the amphipathic peptide helices oriented always preferentially parallel to the interface, independent of the surface pressure in the monolayer. This result was expected for the His-peptide at pH 3, because of its ideal amphipathic helical structure; however, it is surprising that the totally hydrophobic A-peptide also showed little or no tendency toward a perpendicular reorientation, even at high surface pressures. A parallel orientation at the water surface was also proposed for other hydrophobic peptides (Cornell, 1979; Fujita et al., 1974, 1995). Conformation and interfacial orientation of the peptides could be preserved upon LB transfer to gold surfaces, as shown by our RA-FTIR data.

Upon self-assembly on gold, the two peptides oriented differently, thereby indicating the importance of the primary amino acid sequence for the molecular orientation. The more hydrophobic A-peptide adopted a perpendicular orientation. The presence of four histidine and two lysine residues on the same side of the helix was, under our experimental immobilization conditions, sufficient to direct the His-peptides parallel to the surface. It is interesting to note in this context that the His-peptide behaved quite differently at the surface of lipid bilayer membranes in water. Bechinger (1996) has shown that the positively charged, amphipathic His-peptide helices bind to lipid membranes at the interfacial region to the water phase in a parallel orientation. At pH 9 the histidine residues are deprotonated; under this condition the His-peptide helices integrate into and traverse the lipid bilayer. Taking these and our present results together, the orientation of polypeptides at interfacial regions are driven by a finely balanced interaction between the peptides themselves and the contacting bulk phases or surfaces.

The molecular density in immobilized peptide monolayers was controlled by using different layer formation methods, SA and LB transfer. A density of about one peptide molecule per nm^2 was found in self-assembled monolayers of the A-peptide. In the transferred monolayers, the molecular density increased with the pressure of transfer (data not shown), but at a surface pressure of 30 mN/m, it was half that of the self-assembled monolayers. It is interesting to note that the area A_{SPR} of the His-peptide molecules in self-assembled monolayers is distinctly larger than in LB-transferred monolayers. This again indicates that surface charges have an important influence on, and can be used to control, the final peptide density in monomolecular films.

3. In the present work, important information on the orientation of the peptide helices on gold surfaces came from RA-FTIR spectroscopy. Because this technique has not been applied before to peptide monolayers on metallic surfaces, the results presented here deserve closer discussion.

The determination of the orientation of peptide helices was possible because we used two reference systems for calibrating the RA-FTIR spectra of polypeptides: BR and His-peptide layers for perpendicular and parallel interfacial orientations, respectively. For the quantitative evaluation of the helix order parameters, two basic assumptions were necessary: first, that the additional disorder in the peptide layers due to the nonperfect planarity of the gold support, as described by the mosaic spread order parameter S_m in Eq. 10b, is identical for all protein and polypeptide layers (this assumption is obviously reasonable, because identical gold substrates were used in all cases); second, that the internal mobility in the polypeptide backbone leading to conformational fluctuations and flexibility gradients within the BR and the polypeptides are, on the average, identical. To probe this last assumption, MD simulations of monolayers of helical polypeptides were performed. Preliminary results (Cattarinussi, manuscript in preparation) indicate that the internal mobilities of both the A- and the His-peptides are very similar to that of BR in purple membranes (Edholm et al., 1995), thus justifying the assumption made in applying Eq. 10b. Details of these MD results will be published elsewhere.

In our procedure for evaluating orientational molecular order parameters, we used certain assumptions on the IR-

active transition moment orientations with respect to the molecular axis, based on published values (Goormaghtigh et al., 1994a). We believe that the major source of uncertainty introduced by using explicit amide transition moment orientations in α-helices stems from the fact that neither the degree of oriented molecules nor the internal static or dynamic structural disorder is considered. Because the deviation from an ideal α-helical structure due to disorder or intramolecular dynamic fluctuations changes the hydrogen bonding network of the peptide bonds, this effect will have considerable consequences for the optical properties of amide I and amide II, especially on their wavenumber position (maximum intensity and widths of corresponding bands) and the orientational distribution of transition moments. Structural experimental studies (diffraction techniques, NMR, and fluorescence spectroscopy), in combination with molecular dynamics calculations, have shown that deviations from ideal α-helix (as well as β-strand) protein structures represent the rule rather than the exception. Conformational fluctuations within proteins and polypeptide helices show considerable variation, depending on the particular overall structure and environment. Therefore, the orientation of the infrared amide transition moments should also be taken as peptide- and protein-specific parameters that might adopt different values, depending on the properties of each particular system.

Taken altogether, the present work has delivered three major results on the formation of self-organized peptide layers:

1. Stable peptide monolayers of predefined molecular properties can be created at several types of interfaces.

2. The monolayer structure can be controlled by the polypeptide's amino acid composition, the technique used for layer formation, and the supporting surface properties.

3. RA-FTIR measurements in combination with SPR and Langmuir film balance techniques have delivered for the first time direct experimental evidence for the molecular conformation and orientation of pure peptide monolayers. We believe that self-organized polypeptide layers are of general importance for the future development of supramolecular structures for creating new functionalities at interfaces. The formation of such interfaces is of interest for the design of novel materials and artificial receptors, as well as for the understanding of the folding of proteins by self-organization.

We are greatly indebted to the following colleagues, without whose help this work would not have been possible in the present form: Tatsunori Sato and Manfred Mutter for the synthesis of the A-peptide; Burkhard Bechinger for delivering the His-peptide; Wolfgang Gärtner for the gift of BR; and Bernard Desbat for the continuous help, support, and many helpful discussions during the PM-IRRAS experiments that have been performed in his Laboratory at the University of Bordeaux. We are grateful to Serge Cattarinussi for the structural peptide models of Fig. 2 and for giving us access to his MD calculations. We also benefited from discussions with Claus Duschl.

This work was financially supported by the board of the Swiss Federal Institutes of Technology (Priority Program MINAST: 7.06).

REFERENCES

Allara, D. L., A. Baca, and C. A. Pryde. 1978. Distortions of band shapes in external reflection infrared spectra of thin polymer films on metal substrates. *Macromolecules.* 11:1215–1220.

Allara, D. L., and R. G. Nuzzo. 1985. Spontaneously organized molecular assemblies. 2. Quantitative IR spectroscopic determination of equilibrium structures of solution-adsorbed *n*-alcanoic acids on an oxidized aluminum surface. *Langmuir.* 1:52–66.

Bechinger, B. 1996. Towards membrane protein design: pH-sensitive topology of histidine-containing polypeptides. *J. Mol. Biol.* 263:768–775.

Blasie, J. K. 1994. Structure of integral membrane proteins within membranes via X-ray and neutron diffraction: from oriented multilayers to a single monolayer. *In* Membrane Protein Structure. S. H. White, editor. Oxford University Press, New York. 268–280.

Blaudez, D., T. Buffeteau, J. C. Cornut, B. Desbat, N. Escafre, M. Pezolet, and J. M. Turlet. 1994. Polarization modulation FTIR spectroscopy at the air/water interface. *Thin Solid Films.* 242:146–150.

Blaudez, D., J. M. Turlet, J. Dufourcq, T. Buffeteau, and B. Desbat. 1996. Investigations at the air/water interface using polarization modulation IR spectroscopy. *J. Chem. Soc. Faraday Trans.* 92:525–530.

Boncheva, M., C. Duschl, W. Beck, G. Jung, and H. Vogel. 1996. Formation and characterization of lipopeptide layers at interfaces for the molecular recognition of antibodies. *Langmuir.* 12:5636–5642.

Brandrup, J., and E. H. Immergut, editors. 1989. Polymer Handbook, 3rd Ed. Wiley-Interscience, New York. VII-469.

Brooks, B., R. Bruccoleri, B. Olafson, D. J. States, S. Swaminathan, and M. Karplus. 1983. CHARMM: a program for macromolecular energy, minimization and dynamics calculations. *J. Comp. Chem.* 4:187–217.

Brooks, C. L., A. Brunger, and M. Karplus. 1985. Active site dynamics in protein molecules: a stochastic boundary molecular-dynamics approach. *Biopolymers.* 24:843–865.

Cantor, C. R., and P. R. Schimmel. 1980. Biophysical Chemistry, Vol. 2, Table 8-6, 471. W. H. Freeman, San Francisco.

Cevc, G., and D. Marsh. 1987. Phospholipid Bilayers: Physical Principles and Models. J. Wiley and Sons, New York. 347–368.

Chakrabartty, A., J. A. Schellman, and R. L. Baldwin. 1991. Large differences in the helix propensities of alanine and glycine. *Nature.* 351: 586–588.

Chen, Y. H., J. T. Yang, and K. H. Chau. 1974. Determination of the helix and β form of proteins in aqueous solution by circular dichroism. *Biochemistry.* 13:3350–3359.

Cornell, D. 1979. Circular dichroism of polypeptide monolayers. *J. Colloid Interface Sci.* 70:167–180.

Cornut, I., B. Desbat, J. M. Turlet, and J. Dufourcq. 1996. In situ study by polarization modulated FTIR spectroscopy of the structure and orientation of lipids and amphipathic peptides at the air/water interface. *Biophys. J.* 70:305–312.

Debe, M. K. 1982–1983. Organic-metal interface studies with reflection-absorption IR spectroscopy: photomasked surfactants and organic photoconductors on aluminum. *Appl. Surf. Sci.* 14:1–40.

Debe, M. K. 1984. Extracting physical structure information from thin organic films with reflection-absorption IR spectroscopy. *J. Appl. Phys.* 55:3354–3366.

DeGrado, W. F., and J. D. Lear. 1990. Conformational constrained α-helical peptide models for protein ion channels. *Biopolymers.* 29:205–213.

Drexler, K. E. 1992. Nanosystems: Molecular Machinery, Manufacturing, and Computation. Wiley-Interscience, New York.

Duschl, C., A.-F. Sevin-Landais, and H. Vogel. 1996. Surface engineering: optimization of antigen presentation in self-assembled monolayers. *Biophys. J.* 70:1985–1995.

Edholm, O., O. Berger, and F. Jähnig. 1995. Structure and fluctuations of bacteriorhodopsin in the purple membrane: a molecular dynamics study. *J. Mol. Biol.* 250:94–111.

Fendler, J. H. 1994. Membrane-Mimetic Approach to Advanced Materials. Springer Verlag, Berlin.

Fringeli, U. P., and H. H. Günthard. 1981. Infrared membrane spectroscopy. *In* Membrane Spectroscopy. E. Grell, editor. Springer Verlag, New York. 270–332.

Fujita, K., S. Kimura, Y. Imanashi, E. Rump, and H. Ringsdorf. 1994. Monolayer properties of hydrophobic α-helical peptides having various end groups at the air/water interface. *Langmuir.* 10:2731–2735.

Fujita, K., S. Kimura, Y. Imanashi, E. Rump, and H. Ringsdorf. 1995. Two-dimensional assembly formation of hydrophobic helical peptides at the air/water interface: fluorescence microscopic study. *Langmuir.* 11: 253–258.

Fukushima, D., J. P. Kupferberg, S. Yokoyama, D. J. Kroon, E. T. Kaiser, and F. J. Kézdy. 1979. A synthetic amphiphilic helical docosapeptide with the surface properties of plasma apolipoprotein A-I. *J. Am. Chem. Soc.* 101:3703–3704.

Gennis, R. B. 1989. Biomembranes: Molecular Structure and Function. Springer Verlag, New York. 94.

Ghadiri, M., and M. A. Case. 1993. De novo design of a novel heterodinuclear three-helix bundle metalloprotein. *Angew. Chem. Int. Ed. Engl.* 32:1595–1597.

Goormaghtigh, E., V. Cabiaux, and J. M. Ruysschaert. 1994a. Determination of soluble and membrane protein structure by FTIR spectroscopy. I. Assignments and model compounds. *In* Subcellular Biochemistry, Vol. 23. G. B. Ralston and H. J. Hilderson, editors. Plenum Press, New York. 329–362.

Goormaghtigh, E., V. Cabiaux, and J. M. Ruysschaert. 1994b. Determination of soluble and membrane protein structure by FTIR spectroscopy. II. Experimental aspects, side chain structure and H/D exchange. *In* Subcellular Biochemistry, Vol. 23. G. B. Ralston and H. J. Hilderson, editors. Plenum Press, New York. 363–403.

Greenler, R. G. 1966. IR study of adsorbed molecules on metal surfaces by reflection techniques. *J. Chem. Phys.* 44:310–315.

Grigorieff, N., T. A. Ceska, K. H. Downing, J. M. Baldwin, and R. Henderson. 1996. Electron-crystallographic refinement of the structure of bacteriorhodopsin. *J. Mol. Biol.* 259:393–421.

Haris, P. I., and D. Chapman. 1988. FTIR spectra of the polypeptide alamethicin and a possible structural similarity with bacteriorhodopsin. *Biochim. Biophys. Acta.* 943:375–380.

Haris, P., and D. Chapman. 1995. The conformational analysis of peptides using FTIR. *Biopolymers.* 37:251–263.

Jackson, J. D. 1975. Additional theorem for spherical harmonics. *In* Classical Electrodynamics, 2nd Ed. John Wiley and Sons, New York.

Jakobsen, R. J., and F. M. Wasacz. 1987. Effects of environment on structure of adsorbed proteins: FTIR studies. *In* Proteins at Interfaces: Physicochemical and Biochemical Studies. J. L. Brash and T. A. Horbett, editors. American Chemical Society, Washington, DC. 339–361.

Jakobsen, R. J., F. M. Wasacz, and K. B. Smith. 1985. Biological FT-IR: Industrial applications of infrared spectroscopy. *In* Chemical, Biological and Industrial Applications of Infrared Spectroscopy. J. R. During, editor. John Wiley, New York. 199–213.

Krimm, S., and W. C. Reisdorf. 1994. Understanding normal modes of proteins. *Faraday Discuss.* 99:181–197.

Kuhn, H. 1989. Present status and future prospects of Langmuir-Blodgett film research. *Thin Solid Films.* 178:1–16.

Langmuir, I., and V. J. Schäfer. 1938. Activities of urease and pepsin monolayers. *J. Am. Chem. Soc.* 60:1351–1360.

Lyddane, R. H., R. D. Sachs, and E. Teller. 1941. On the polar vibrations of alkali halides. *Phys. Rev.* 59:673–676.

Lyu, P. C., M. I. Liff, L. A. Marki, and N. R. Kallenbach. 1990. Side chain contributions to the stability of alpha-helical structure in peptides. *Science.* 250:669–673.

MacRitchie, F. 1987. Consequences of protein adsorption at fluid interfaces. *In* Proteins at Interfaces: Physicochemical and Biochemical Studies. J. L. Brash and T. A. Horbett, editors. American Chemical Society, Washington, DC. 165–179.

Meseth, U. 1996. Structural and functional investigation of channel-forming peptides in lipid membranes. Ph.D. thesis. EPF-Lausanne, Switzerland.

Mielczarski, J. A. 1993. External reflection IR spectroscopy at metallic, semiconductor and nonmetallic substrates. 1. Monolayer films. *J. Phys. Chem.* 97:2649–2663.

Minor, D. L. J., and P. S. Kim. 1994. Measurement of the beta-sheet-forming propensities of amino acids. *Nature.* 367:660–663.

Mrksich, M., and G. M. Whitesides. 1996. Using self-assembled monolayers to understand the interactions of man-made surfaces with proteins and cells. *Annu. Rev. Biophys. Biomol. Struct.* 25:55–78.

Porter, M. D., T. B. Bright, D. L. Allara, and C. E. D. Chidsey. 1987. Spontaneously organized molecular assemblies. 4. Structural characterization of *n*-alkyl thiol monolayers on gold by optical ellipsometry, IR spectroscopy and electrochemistry. *J. Am. Chem. Soc.* 109:3559–3568.

Prime, K. L., and G. M. Whitesides. 1991. Self-assembled organic monolayers: model systems for studying adsorption of proteins at surfaces. *Science.* 252:1164–1167.

Rothschild, K. J., and N. A. Clark. 1979. Polarized infrared spectroscopy of oriented purple membrane. *Biophys. J.* 25:473–488.

Schmitt, L., T. Bohanon, S. Denzinger, H. Ringsdorf, and R. Tampé. 1996. Specific protein docking to chelator lipid monolayers monitored by FTIR spectroscopy at the air/water interface. *Angew. Chem. Int. Ed. Engl.* 35:317–320.

Schneider, J. P., and J. W. Kelly. 1995. Templates that induce α-helical, β-sheet, and loop conformations. *Chem. Rev.* 95:2169–2187.

Schwarz, G., and S. E. Taylor. 1995. Thermodynamic analysis of the surface activity exhibited by a largely hydrophobic peptide. *Langmuir.* 11:4341–4346.

Smith, L. J., and D. C. Clark. 1992. Measurement of the secondary structure of adsorbed protein by circular dichroism. 1. Measurements of the helix content of adsorbed melittin. *Biochim. Biophys. Acta.* 1121: 111–118.

Sober, H. E., editor. 1973. Handbook of Biochemistry. CRC Press, Cleveland, OH. C-67.

Song, Y. P., M. C. Petty, J. Yarwood, W. J. Feast, J. Tsibouklis, and S. Mukherjee. 1992. FTIR studies of molecular ordering and interactions in LB films containing nitrostilbene and stearic acid. *Langmuir.* 8:257–261.

Surewicz, W. K., H. H. Mantsch, and D. Chapman. 1993. Determination of protein structure by FTIR spectroscopy: a critical assessment. *Biochemistry.* 32:389–394.

Terretaz, S., T. Stora, C. Duschl, and H. Vogel. 1993. Protein binding to supported lipid membranes: investigation of the cholera toxin-ganglioside interaction by simultaneous impedance spectroscopy and surface plasmon resonance. *Langmuir.* 9:1361–1369.

Thiaudière, E., M. Soekarjo, E. Kuchinka, A. Kuhn, and H. Vogel. 1993. Structural characterization of membrane insertion of M13 procoat, M13 coat, and Pf3 coat proteins. *Biochemistry.* 32:12186–12196.

Torii, H., and M. Tasumi. 1996. Theoretical analyses of the amide I infrared bands of globular proteins. *In* Infrared Spectroscopy of Biomolecules. D. Chapman and H. Mantsch, editors. Wiley-Liss, New York. 1–18.

Trissl, H.-W., and W. Gärtner. 1987. Rapid charge separation and bathochromic absorption shift of flash-excited bacteriorhodopsins containing 13-*cis* or all-*trans* forms of substituted retinals. *Biochemistry.* 26: 751–758.

Tuchscherer, G., and M. Mutter. 1995. Templates in protein de novo design. *J. Biotechnol.* 41:197–210.

Ulman, A. 1991. An Introduction to Ultrathin Organic Films: From Langmuir-Blodgett to Self-Assembly. Academic Press, San Diego.

Urry, D. W. 1993. Molecular machines: how motion and other functions of living organisms can result from reversible chemical changes. *Angew. Chem. Int. Ed. Engl.* 32:819–841.

Vogel, H., and W. Gärtner. 1987. The secondary structure of bacteriorhodopsin determined by Raman and circular dichroism spectroscopy. *J. Biol. Chem.* 262:11464–11469.

Vogel, H., L. Nilsson, R. Rigler, S. Meder, G. Boheim, W. Beck, H.-H. Kurth, and G. Jung. 1993. Structural fluctuations between two conformational states of a transmembrane helical peptide are related to its channel-forming properties in planar lipid membranes. *Eur. J. Biochem.* 212:305–313.

Vogel, H., L. Nilsson, R. Rigler, K.-P. Voges, and G. Jung. 1988. Structural fluctuations of a helical polypeptide traversing a lipid bilayer. *Proc. Natl. Acad. Sci. USA.* 85:5067–5071.

Whitesell, J. K., H. K. Chang, and C. S. Whitesell. 1994. Enzymatic grooming of organic thin films. *Angew. Chem. Int. Ed. Engl.* 33: 871–873.

Wöhr, T., F. Wahl, A. Nefzi, B. Rohwedder, T. Sato, X. Sun, and M. Mutter. 1996. Pseudo-prolines as a solubilizing, structure-disrupting protection technique in peptide synthesis. *J. Am. Chem. Soc.* 118: 9218–9227.

Yen, Y.-S., and J. S. Wong. 1989. Infrared reflectance properties of surface thin films. *J. Phys. Chem.* 93:7208–7216.